Soils and Rocks
An International Journal of Geotechnical and Geoenvironmental Engineering
www.soilsandrocks.com
ISSN 1980-9743
ISSN-e 2675-5475

Estimating soil water retention curve in tropical residual soils: a comparative study of measurement and modeling techniques

João Vitor Almeida Leite[1#], Vinícius Samahá Salles[1],
Mariana Ferreira Benessiuti Motta[1], Marcio Roberto Magalhães de Andrade[2],
Daniel Metodiev[2]

Article

Keywords
Residual soils
Laboratory tests
Inverse modeling
Mercury intrusion porosimetry
Pedotransfer functions
Dual porosity

Abstract

This study evaluates various methods for estimating soil water retention curves (SWRCs) in tropical residual soils from the Baixada Santista region, Brazil, including both young and mature profiles. Laboratory data were obtained using HYPROP, WP4C, and the filter paper method, and curve fitting was performed using unimodal and bimodal van Genuchten models. The estimates were derived from mercury intrusion porosimetry (MIP), pedotransfer functions (PTF-SV and PTF-Bi), and inverse modeling with Hydrus-1D, using field moisture and rainfall data from CEMADEN. Model performance was assessed using RMSE, MAE, MBE, and correlation coefficients. For mature soils, PTF-SV showed the best statistical performance but failed to represent bimodal structure. In contrast, PTF-Bi and MIP better reflected dual porosity but with higher errors. For young soils, Hydrus-1D produced the best fit, especially in simpler pore systems. Although the models showed a strong correlation with laboratory data, they often yielded divergent van Genuchten parameters, indicating that statistical agreement does not necessarily ensure an accurate physical representation. No method consistently outperformed others across all soil types. These findings highlight the influence of soil structure and calibration data on model reliability and reinforce the need to develop tailored approaches for Brazilian tropical soils with complex hydraulic behavior.

1. Introduction

Understanding the hydraulic behavior of unsaturated soils is essential for various applications in geotechnical engineering, particularly in regions prone to extreme events such as landslides. Among the main properties in this context is the soil water retention curve (SWRC), which describes the relationship between soil moisture content and suction. SWRC is widely used to simulate water flow in unsaturated porous media, assess soil water storage capacity, and predict slope stability, for instance (Durner, 1994; Fredlund & Xing, 1994; Zhuang et al., 2024).

Despite its importance, accurately characterizing SWRC remains a technical challenge in weathered tropical soils, such as those found in the Baixada Santista region of the state of São Paulo, Brazil. This region is predominantly composed of young and mature residual soils with heterogeneous structures, dual porosity, and high water retention capacities, which complicates the direct application of models developed for temperate-region soils (Tomasella et al., 2000; Ottoni et al., 2018; Mendes & Marinho, 2020).

This hydraulic property is difficult to measure and determine, and various direct and indirect techniques have been employed to obtain SWRC. Traditional laboratory methods, such as the filter paper technique and pressure plate apparatus, are often supplemented by more advanced approaches such as the HYPROP and WP4C systems, which allow for continuous and high-resolution data acquisition across different suction ranges (Zhuang et al., 2024; Schindler & Müller, 2017; Singh et al., 2020; Singh & Verdi, 2024).

Given that laboratory tests are time-consuming and labor-intensive, many studies have adopted estimation methods for the retention curve. Among these, mercury intrusion porosimetry (MIP) has been explored as a supplementary technique to estimate SWRC, especially in soils with aggregated or bimodal structures, such as weathered tropical soils. MIP enables the inference of pore-size distribution, and when combined with empirical models such as the van Genuchten model, can aid in modeling hydraulic behavior (Mendes & Marinho, 2020; Delcourt et al., 2022; Satyanaga et al., 2024).

Predictive models have also gained prominence. Pedotransfer functions (PTFs) based on machine learning, such

#Corresponding author. E-mail address: jva.leite@unesp.br
[1]Universidade Estadual Paulista "Júlio de Mesquita Filho", Faculdade de Engenharia, Departamento de Engenharia Civil, Guaratinguetá, SP, Brasil.
[2]Centro Nacional de Monitoramento e Alertas de Desastres Naturais, São José dos Campos, SP, Brasil.

Submitted on October 22, 2025; Final Acceptance on March 31, 2026; Discussion open until November 30, 2026.
Editor: Renato P. Cunha
https://doi.org/10.28927/SR.2026.017425

as the pseudo-continuous neural network PTF (PCNN-PTF) proposed by Singh & Verdi (2024), and the bimodal function by Pereira et al. (2024), have shown superior performance in predicting SWRC by incorporating physical variables such as texture, bulk density, and plasticity index. These models have shown promising results but still require further validation in tropical soils, as their training datasets are typically based on temperate or subtropical soils (Tomasella et al., 2000; Ottoni et al., 2018; Pereira et al., 2024; Singh et al., 2020; Singh & Verdi, 2024; Albuquerque et al., 2022).

Moreover, inverse modeling using the Hydrus-1D software has proven to be a powerful tool for estimating hydraulic parameters based on field data (Le Bourgeois et al., 2016; Filipović et al., 2018; Ket et al., 2018). This technique is especially useful in instrumented areas equipped with moisture sensors, enabling the calibration of water retention curves using actual moisture and rainfall data. The approach involves estimating a limited set of unknown model parameters using easily measurable variables (model output), which are compared with observations through the optimization of the objective function (Ket et al., 2018).

In this context, the present study aims to evaluate different methods for estimating the soil water retention curve in residual soils from the Baixada Santista region, encompassing profiles of young and mature residual soils. Laboratory tests were performed using the HYPROP and WP4C equipment and the filter paper technique, followed by curve fitting with the van Genuchten models in both unimodal and bimodal forms (Durner, 1994; van Genuchten, 1980; Seki et al., 2023). In addition, data from moisture sensors installed down to three meters depth and pluviometers provided by CEMADEN (National Center for Monitoring and Early Warning of Natural Disasters) were used for inverse modeling with Hydrus-1D, alongside MIP analyses and application of PTFs (Pereira et al., 2024; Singh & Verdi, 2024). The accuracy of the methods was assessed using statistical metrics. It is expected to contribute to the advancement of knowledge on the hydraulic characterization of tropical residual soils and support the development of representative predictive models that reflect their specificities.

2. Materials and methods

2.1 Testing soil horizons

The study sites are located in the Baixada Santista region, on the coast of the state of São Paulo, Brazil, specifically in the Jardim Albamar Condominium, in the municipality of Guarujá (−23.948512°, −46.170522°), and in the Xixová-Japuí State Park, in São Vicente (−23.982131°, −46.380465°). This region lies along isolated hills and narrow mountains distributed along the coastal area adjacent to the Serra do Mar escarpment, composed of polydeformed Precambrian crystalline rocks covered by mantles of weathered soil, a product of the high temperatures and rainfall of the dominant humid tropical climate.

The rock surfaces are highly irregular, displaying pronounced domal features due to exfoliation processes. A well-developed joint system with diaclases is also observed, facilitating water infiltration and promoting differential weathering of more fragile minerals. This condition favors, over time, the development of thick soil profiles and the potential initiation of shallow landslides.

Two profiles were selected for this investigation at each site (Guarujá – GJ and São Vicente – SV) – Figure 1. Undisturbed and disturbed samples were specifically collected with the aim of determining soil water retention curves and improving the understanding of subsurface hydraulic behavior in risk-prone areas. The samples were collected at the same depths as the soil moisture sensors installed in the field, allowing for a direct comparison between laboratory-derived hydraulic parameters and in situ moisture dynamics.

Four representative samples from the two profiles were selected for study: GJM (Guarujá – mature residual soil), GJY (Guarujá – young residual soil), SVM (São Vicente – mature residual soil), and SVY (São Vicente – young residual soil), encompassing two geological settings and two weathering stages. The objective was not statistical generalization, but a detailed comparative assessment of SWRC estimation methods under well-characterized tropical residual soil conditions.

The parent rock of the residual soil samples corresponds to migmatitic gneisses of granitoid composition. At São Vicente, these rocks exhibit quartz-feldspathic and mafic banding, while porphyroid varieties, such as augen gneisses, are found at Guarujá (CPRM, 2006). The mature residual soil is relatively homogeneous and shallow. It has a granular framework composed of quartz grains and a matrix of low-compressibility clay. The young residual soil is heterogeneous, micaceous and contains embedded small rock fragments.

The classification of tropical residual soils poses significant challenges due to their complex genesis, microstructure, and hydraulic behavior. The weathering of metamorphic crystalline rocks, characterized by varied compositional banding and polydeformational structures, directly influences the framework and composition of residual soil profiles, especially on hillslopes. Mature soils in particular are often cemented by high concentrations of iron and aluminum oxides and exhibit varying degrees of aggregation, which strongly influence their SWRCs and pore size distributions (Tomasella et al., 2000; Alves et al., 2025).

Table 1 shows the results of the physical characterization tests of these materials. Geotechnical characterization tests were performed following the Brazilian Association of Technical Standards/ABNT (ABNT, 2016a, b; ABNT, 2022; ABNT, 2025a, b).

Figure 2 shows the results of the incremental pore size distribution obtained by mercury intrusion porosimetry (MIP).

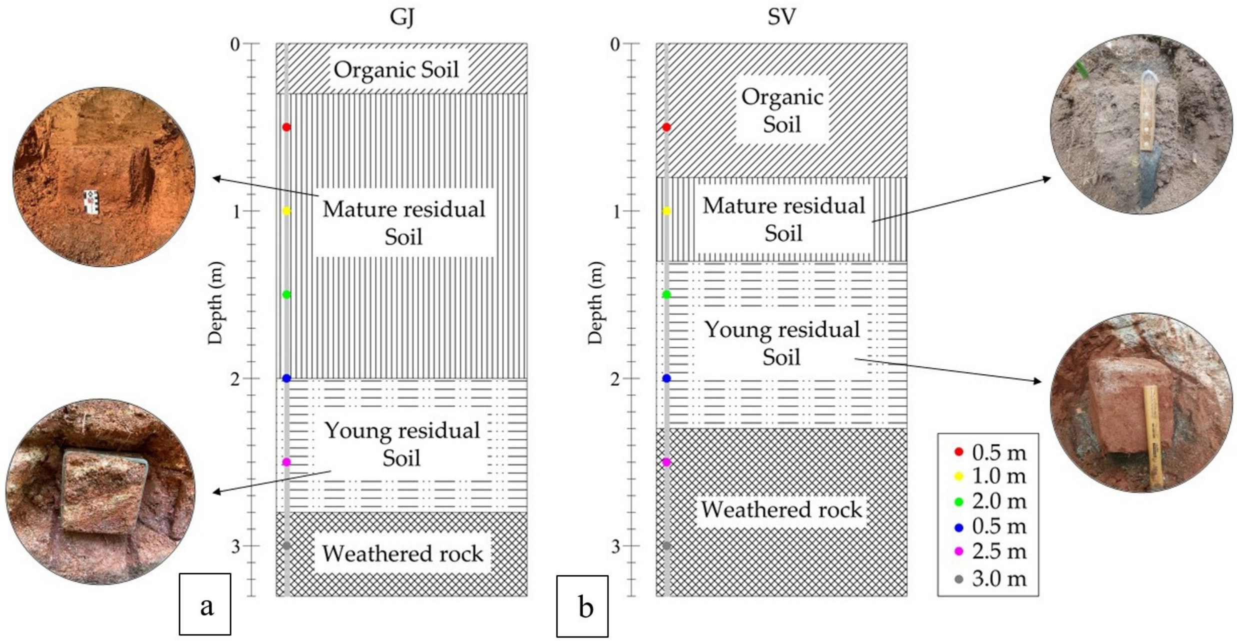

Figure 1. Schematic representation of the soil profiles and soil moisture sensors for the study sites in: (a) Guarujá (GJ); (b) São Vicente (SV).

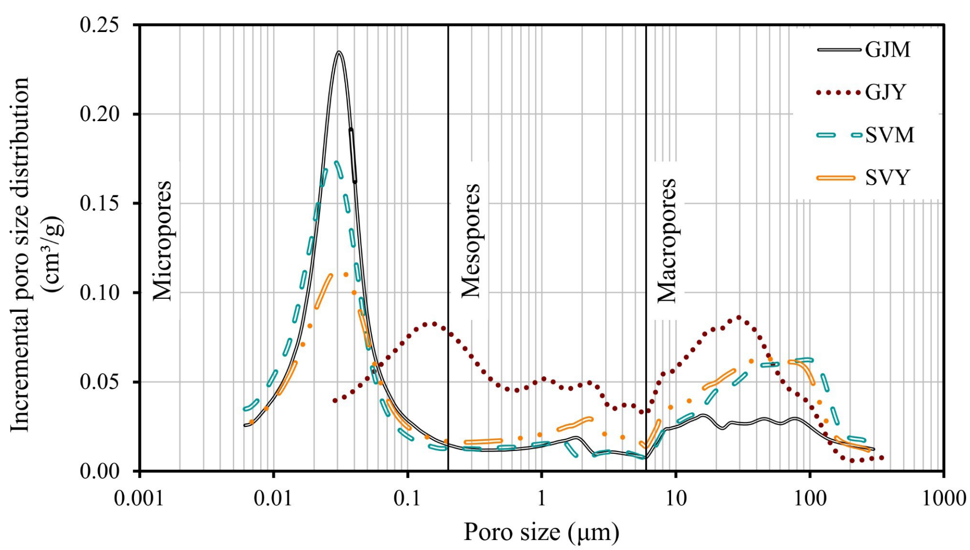

Figure 2. Incremental pore size distribution of the studied soils.

Table 1. Physical characterization results and average index properties.

Physical properties	SVM	GJM	SVY	GJY
Grain size distribution (with deflocculant)				
Gravel (%) – 2<φ<60 mm	0.8	0.6	2.0	1.0
Sand (%) – 0.06<φ<2 mm	64.1	51.0	66.0	53.6
Silt (%) – 0.002<φ<0.6 mm	23.0	29.4	25.1	34.1
Clay (%) – φ<0.002 mm	12.0	19.0	6.9	11.3
USCS	SM	ML	SM	SM

Legend: see List of Symbols.

Table 1. Continued...

Physical properties	SVM	GJM	SVY	GJY
Grain size distribution (with deflocculant)				
Grain size distribution (without deflocculant)				
Gravel (%) – 2<φ<60 mm	0.8	0.6	NM	NM
Sand (%) – 0.06<φ<2 mm	85.7	87.6	NM	NM
Silt (%) – 0.002<φ<0.6 mm	13.5	11.8	NM	NM
Clay (%) – φ<0.002 mm	0.0	0.0	NM	NM
USCS	SM	SM	-	-
Index properties				
G_S	2.737	2.663	2.618	2.640
w_i (%)	23.55	29.71	22.49	22.41
e_i	1.27	0.92	1.14	1.16
S_i (%)	43.40	86.45	50.88	55.16
n (%)	55.90	47.70	53.20	53.20
γ_d (kN/m^3)	11.48	13.64	12.85	12.07
Atterberg Limits				
w_L (%)	39	37	-	-
w_P (%)	NP	26	NP	NP

Legend: see List of Symbols.

Based on Camapum de Carvalho & Gitirana Junior (2021) and Delcourt et al. (2022), the typical physical–microstructural patterns observed in tropical residual soils, SVM and GJM are highly weathered residual soils, representative of the mature horizon. Their fine-textured matrix is rich in aggregated micropores, while macropores are present in smaller quantities but still form a distinct domain in the SWRC. This dual arrangement produces a bimodal soil water retention curve, with a first drainage step at low suctions associated with macropore emptying and a second at higher suctions linked to micropore desaturation.

In contrast, SVY and GJY represent younger residual materials. They retain some mineral alignment and relic features from the parent rock, resulting in a more heterogeneous pore network. The pore size distribution is dominated by macropores and mesopores, with a smaller contribution from micropores.

2.2 Laboratory measurements

Soil water retention curves for the four soil samples were determined using three methods: the combination of the evaporation method (HYPROP) and psychrometry (WP4C), and the filter paper method.

The first method used HYPROP for lower suction values (0 to 100 kPa) and WP4C for higher values (200 to 150,000 kPa), similar to the procedure adopted by Maček et al. (2013). The test procedure followed the manufacturer's guidelines (METER Group, 2025a, b). Zhuang et al. (2017) explained that during Hyprop tests, the top surface of the sample is exposed to air to promote evaporation, while the balance records evaporation rates, allowing the water content to be derived from the weight of the setup and the pressure readings. The test ends when the tension in the soil around the tensiometers exceeds the air entry pressure of the ceramic material, causing the measured matric potential to drop to zero (Haghverdi et al., 2018).

After completing the test, the samples were collected for use in the WP4C device. This equipment enables the measurement of total matric potential during the equilibrium process between the liquid and vapor phases of water in a sealed chamber (Bittelli & Flury, 2009; Solone et al., 2012).

Finally, the filter paper method allowed determining the soil matric suction over a range from 4 to 35,000 kPa, following ASTM D5298 (ASTM, 2016). Soil suction was indirectly estimated based on the final water content of the filter paper (Whatman No. 42) and its calibration curve, assuming equilibrium between the soil and the paper, after drying path (Motta, 2016).

Although the combined HYPROP-WP4C system covers a wide suction range, each technique has operational limitations. HYPROP is reliable at low suctions (0 – 100 kPa) but may be affected by cavitation near the ceramic air-entry value. WP4C performs better at higher suctions, with increased uncertainty near saturation. The filter paper method covers a broad range; however, as an indirect technique, it is sensitive to calibration and testing conditions, which may introduce variability.

To balance the influence of experimental methods with varying data densities (HYPROP, WP4C, and Filter Paper), a weighting scheme for experimental points was implemented during curve fitting. First, a global weight inversely proportional to the number of points per test was assigned, equalizing the total significance of each technique. Subsequently, a local weight was applied within the logarithmic suction domain. The local weight for each data point is proportional to the average distance to its immediate neighbors. This minimizes redundancy in high-density clusters and prioritizes isolated points that define the curve's slope, ensuring an unbiased parameter estimation across the entire suction range.

The fitting procedures were performed using SWRC-FIT (Seki et al., 2023), in which all available constitutive models were tested. The final model selection was based on the highest coefficient of determination (R^2), overall fitting consistency, and physical coherence of the estimated parameters. From this comparative evaluation, the van Genuchten unimodal model (VG) provided the best representation for the young soils, whereas the bimodal van Genuchten model (dual-VG) more accurately captured the structural heterogeneity of the mature soils.

Although alternative formulations are available, the van Genuchten model was considered suitable for the objectives of this study. Moreover, most predictive and numerical models employed herein are formulated based on the van Genuchten parameterization. Its adoption therefore ensures methodological consistency, facilitates parameter estimation and comparison, and avoids the need for parameter transformation between different constitutive formulations.

The van Genuchten (VG) model, adopted for the young residual soil, represents a unimodal hydraulic model (van Genuchten, 1980). The model is expressed as:

$$S_e = \left[\frac{1}{1+(\alpha h)^n}\right]^m, \ m = 1 - \frac{1}{n} \tag{1}$$

$$\theta(h) = \theta_r + (\theta_s - \theta_r) S_e \tag{2}$$

where θ is the volumetric water content at matric potential h, θ_s and θ_r are the saturated and residual water contents, respectively, S_e is the effective water saturation, and α and n are parameters that define the curve shape (Singh & Verdi, 2024).

However, a dual-porosity van Genuchten model (dual-VG), applied to the mature residual soil, exhibits bimodal characteristics (Durner, 1994; Zhuang et al., 2024; Priesack & Durner, 2006):

$$S_e = w_1 \left[1+(\alpha_1 h)^{n_1}\right]^{-m_1} + (1-w_1) \left[1+(\alpha_2 h)^{n_2}\right]^{-m_2}, \ m_i = 1 - \frac{1}{n_i} \tag{3}$$

where w_i (i = 1, 2) are weighting factors associated with macropore and micropore domains, and α_i and n_i are parameters that define the shape of the bimodal curve.

The van Genuchten parameters were interpreted according to their physical meaning. The parameter α is related to the air-entry suction and dominant pore size, n to the pore-size distribution and structural uniformity, and, in the bimodal model, w_1 to the relative contribution of macro- and micropore domains. This interpretation supported the assessment of parameter consistency with the expected structural characteristics of the studied residual soils.

It is important to note that hysteresis effects in the soil water retention curve were not explicitly considered in this study. All retention data were obtained under drying conditions, which correspond to the desorption path of the soil water retention curve. This consideration is justified as the comparison among methods required uniform conditions, and most predictive models and pedotransfer functions applied in this study do not explicitly incorporate hysteresis in their formulations.

2.3 Mercury intrusion porosimetry tests

As previously discussed, MIP is a valuable technique for investigating soil microstructure and pore size distribution. The test involves injecting mercury into an undisturbed sample previously dried under controlled pressure. Air-drying was adopted to ensure air-filled pores while minimizing potential microstructural disturbance that may occur under oven-drying conditions.

The technique enables estimation of the drying soil water retention curve, as the excess pressure required for mercury intrusion into an air-filled sample is analogous to the air-entry process in a saturated soil (Prapaharan et al., 1985). The cumulative volume of injected mercury is converted into the apparent degree of saturation (Mendes & Marinho, 2020), assuming that the total void volume equals the total intruded mercury volume. This approach assumes full pore accessibility and neglects ink-bottle effects and occluded porosity.

To derive SWRCs, the relationship between mercury intrusion (a non-wetting fluid) and air-induced water displacement (a wetting fluid) for equivalent pore diameters was adopted (Delcourt et al., 2022; Aung et al., 2001). This conversion follows the methodology described by Delcourt et al. (2022). The pore diameter–suction relationship for water is obtained from the Laplace equation:

$$u_s = \frac{4T_w \cos(\theta_w)}{D} \tag{4}$$

where θ_w is the contact angle (assumed 180°), T_w is the surface tension (72.75 × 10^{-3} N/m), and D is the pore diameter. Mercury has the expression for the diameter for each corresponding pressure value p:

$$p = \frac{-4T_{nw} \cos(\theta_{nw})}{D^*} \tag{5}$$

where θ_{nw} is equal to 130°, T_{nw} is equal to 485 x 10^{-3} N/m, and D^* is the pore diameter. Thus, assuming $D = D^*$ in Equations 4 and 5:

$$u_s = -\left(\frac{T_w \cos(\theta_w)}{T_{nw} \cos(\theta_{nw})}\right) p = 0.233p \quad (6)$$

This conversion assumes cylindrical pore geometry and constant contact angles and surface tension. The degree of saturation is calculated according to Romero et al. (1999):

$$Sr = (1 - Sr_{nw}) + w_r \frac{Sr_{nw}}{w_S} \quad (7)$$

where w_r is the hygroscopic water content, and w_s is the water content corresponding to the total saturation of the soil sample. Additionally:

$$Sr_{nw} = \frac{n}{n_0} \quad (8)$$

$$n = \rho V_{inj} \quad (9)$$

$$n_0 = 1 - \left(\frac{\rho_d}{\rho_s}\right) \quad (10)$$

where n is the intruded porosity, n_0 is the total soil porosity, ρ is the apparent specific mass, V_{inj} is the volume of mercury injected per unit mass, ρ_d is the apparent dry specific mass, and ρ_s is the specific particle mass.

Thus, SWRC was estimated based on Equations 6 and 7 and used for comparison with the other methods addressed in this study.

2.4 Pedotransfer functions

Pedotransfer functions (PTFs) are models used to estimate the hydraulic properties of soils based on basic variables, such as sand, silt and clay fractions, and apparent density (Singh & Verdi, 2024). Singh et al. (2020) showed that SWRC can be estimated using both parametric and pseudo-continuous PTFs (PC-PTFs). Thus, the complexity involved in obtaining SWRC can be reduced using machine learning-based models, which are trained to recognize the shape of the curve from in situ water retention measurements (Haghverdi et al., 2018).

This study employed the PCNN-PTF, based on artificial neural networks, proposed by Singh & Verdi (2024) (PTF-SV), and the model developed by Pereira et al. (2024) (PTF-Bi). The former showed promising results when compared to the Rosetta model, one of the most widely used and internationally recognized models for estimating SWRC. The mentioned neural network is a three-layer feedforward perceptron, trained using an international database (Schindler & Müller, 2017) and a Turkish dataset (Haghverdi et al., 2018), both obtained through the evaporation method using the HYPROP system. The function uses soil texture, apparent density, and soil suction to estimate the volumetric water content (VWC). Input values for this study were based on those shown in Table 1.

However, since this research focuses on tropical residual soils and mature residual soils exhibit bimodal characteristics, the PTF proposed by Pereira et al. (2024) was applied. This PTF has a database composed mostly of soils from the Midwest region of Brazil, developed to predict the retention curve of bimodal tropical soils. Input parameters include soil texture, obtained by sedimentation tests with and without deflocculant, liquidity limit, and plasticity index. For the prediction, the authors developed two neural networks designed to estimate matric suction and degree of saturation. The network architecture was empirically defined through trial and error, using six and eight neurons, respectively, along with two hidden layers and activation functions: hyperbolic tangent and Rectified Linear Unit (ReLU). The original article provides further detail on the construction of these pedotransfer functions.

2.5 Inverse modeling using HYDRUS-1D

In this study, the HYDRUS-1D software (Šimůnek et al., 1999) was employed to estimate the soil water retention curve (SWRC) parameters through inverse modeling. This procedure is based on the numerical solution of Richards' equation (Richards, 1931), which describes water flow in unsaturated porous media, combined with the van Genuchten–Mualem (van Genuchten, 1980) formulation, widely used to represent the hydraulic behavior of soils with unimodal pore-size distribution. For soil layers exhibiting bimodal pore structure, the dual-porosity formulation proposed by Durner (dual van Genuchten–Mualem model) was adopted to represent the contribution of macro- and micropore domains.

The soil profiles implemented in the software were defined based on field tactile–visual descriptions and subdivided into layers with distinct properties down to a depth of 3.3 m. Soil layer thicknesses were defined according to the previously described soil profiles and were kept fixed during the inverse modeling procedure. For each layer, initial estimates of the hydraulic parameters of the SWRC (θ_r, θ_s, α, and n) and the saturated hydraulic conductivity (K_s) were obtained using the "Rosetta – Contents" pedotransfer function (Schaap et al., 2001), integrated into HYDRUS-1D. This estimation was based on laboratory-determined soil texture (sand, silt, and clay contents) and bulk density. In the soil layers classified as bimodal, the parameters of the secondary domain (w_2, α_2, n_2) were assigned by the authors, since Rosetta does not provide estimates for these parameters.

Water flow boundary conditions were defined according to field conditions. The upper boundary condition was established as a variable pressure head/flux condition driven by measured precipitation data, while free drainage was adopted at the lower boundary. Initial conditions were defined based on volumetric water content measurements taken in the field using Data Collection Platforms (DCPs) sensors.

The simulations were carried out considering field conditions observed in 2024, using hourly rainfall data obtained from rain gauges installed at the DCPs operated by CEMADEN, together with volumetric water content data recorded by capacitive sensors (EnviroScan™) installed at depths of 0.5, 1.0, 1.5, 2.0, 2.5, and 3.0 m, as previously mentioned. Each sensor was assumed to be representative of a corresponding soil layer.

Three days characterized by high rainfall intensity and pronounced variations in soil moisture were selected to enhance model sensitivity in estimating hydraulic parameters, representing a critical scenario for the hydrodynamic behavior of the soil profile. Inverse modeling was performed using the inverse solution module of HYDRUS-1D, considering soil hydraulic parameters (θ_r, θ_s, α, n, and K_s) as optimization variables. Parameter bounds followed the default ranges implemented in HYDRUS-1D to ensure physically meaningful solutions. The inverse calibration process followed the standard weighted least-squares framework, with weighting based on the standard deviation of the measurements, with a maximum of 100 iterations.

Importantly, the entire fitting procedure was based exclusively on field experimental data and the initial parameter estimates provided by Rosetta, without incorporating direct laboratory-measured soil water retention curves. This approach aimed not only to evaluate the applicability of inverse modeling but also to better approximate the estimated hydraulic parameters to actual monitored field conditions.

2.6 Performance assessment

The following statistical metrics were calculated to validate the model that best approximates the experimentally derived soil water retention curve (SWRC): root mean square error (RMSE), mean absolute error (MAE), mean bias error (MBE), and correlation coefficient (R). The respective equations are given by:

$$\text{RMSE} = \sqrt{\frac{1}{n}\sum_{i=1}^{n}\left(\theta_{e,i} - \theta_{m,i}\right)^2} \tag{11}$$

$$\text{MAE} = \frac{1}{n}\sum_{i=1}^{n}\left|\theta_{e,i} - \theta_{m,i}\right| \tag{12}$$

$$\text{MBE} = \frac{1}{n}\sum_{i=1}^{n}\left(\theta_{e,i} - \theta_{m,i}\right) \tag{13}$$

$$R = \frac{\sum_{i=1}^{n}\left(\theta_{e,i} - \overline{\theta_e}\right)\left(\theta_{m,i} - \overline{\theta_m}\right)}{\sqrt{\sum_{i=1}^{n}\left(\theta_{e,i} - \overline{\theta_e}\right)^2 \sum_{i=1}^{n}\left(\theta_{m,i} - \overline{\theta_m}\right)^2}} \tag{14}$$

in which θ_e and θ_m are the estimated and measured volumetric water content, respectively, *e* and *m* are the means of the estimated and measured volumetric water content values and *n* is the number of observations.

3. Analysis and results

3.1 Laboratory SWRC's

The SWRC's obtained for mature residual soils (GJM and SVM) and young residual soils (GJY and SVY) showed significant differences, influenced by the microstructure previously analyzed through MIP. Furthermore, the combination of HYPROP and WP4C, along with the filter paper method, allowed the determination of volumetric water content over a wide suction range. Figure 3 and Table 2 show the results of the experimental tests and the fitting using the van Genuchten model, which incorporates data from all tests (Model Fit).

The Model Fit showed an excellent agreement with the experimental retention data of all soils, with R^2 values above 0.96. This confirms the adequacy of both unimodal and bimodal formulations for representing the hydraulic behavior of residual tropical soils.

According to Qian et al. (2022), bimodal soils frequently generate a SWRC with two distinct desaturation stages separated by a plateau or gently sloping transition zone. The first stage, occurring at low suction values, is typically associated with macropore drainage, while the second stage, at higher suctions, corresponds to micropore desaturation.

The MIP results for GJM and SVM corroborate this interpretation (Figure 2). Both soils exhibit two distinct pore domains in the incremental pore size distribution, with a clear separation between macropores and micropores. In GJM, the macropore domain shows an abrupt drainage at very low suctions, followed by dominant retention in the finer pore fraction, indicating a strongly aggregated structure with significant intra-aggregate microporosity. In contrast, SVM presents a more gradual initial desaturation and a more balanced distribution between macro- and micropores, consistent with a less pronounced structural contrast.

The weighting factors (w_1 = 0.114 for GJM and 0.269 for SVM) indicate distinct macropore and micropore domains. In GJM, the high n_1 value (8.00) and the very low α_2 reflect a sharp air-entry related to structural pores, followed by water release from finer pores. SVM also presented two retention domains, but with less marked contrast, as shown by more moderate n_1 and n_2 values (1.89 and 1.37), consistent with structural aggregation but greater pore continuity.

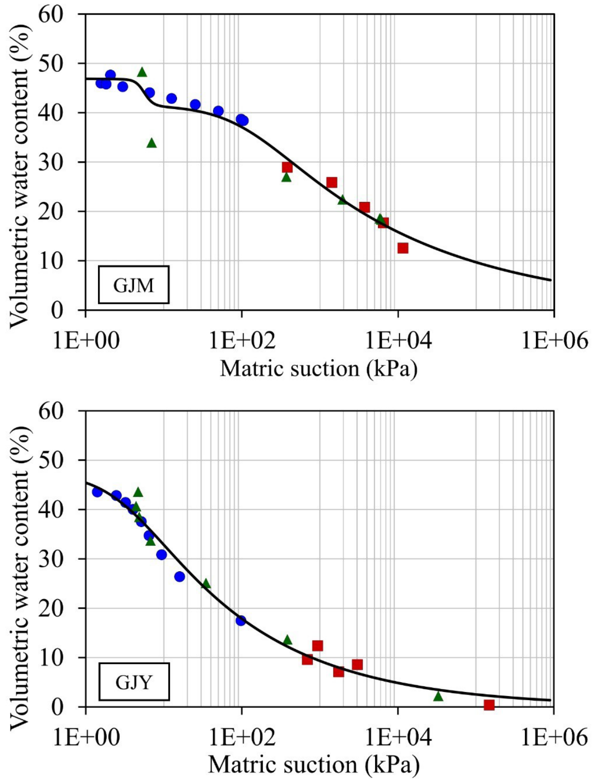

Figure 3. Measured and fitted water retention curves (Model Fit) for the studied soils (GJM, SVM, GJY, and SVY) using two hydraulic models: dual-VG for mature soils and VG for young soils.

Table 2. van Genuchten model fitting parameters obtained from experimental SWRC data.

Model fit	**Soils**			
	GJM	**SVM**	**GJY**	**SVY**
θ_s (%)	46.90	49.24	47.52	38.03
θ_r (%)	0	0	0	0.16
w_1	0.114	0.269	-	-
α_1	1.81E-01	5.01E-01	3.13E-01	5.47E-02
n_1	8	1.89	1.28	1.34
α_2	9.26E-03	4.65E-03	-	-
n_2	1.21	1.37	-	-

In contrast, the GJY and SVY soils show a more gradual and continuous desaturation, commonly expected in unimodal soils (Zhuang et al., 2024). The authors state that water loss occurs progressively over a broad or narrow suction range, depending on the uniformity of pore sizes. Gomes et al. (2023) demonstrated that the slope of the desaturation zone is related to pore size uniformity: a steeper slope corresponds to a more uniform distribution, while a gentler slope indicates greater variability in pore sizes. Both soils presented relatively low *n* values (1.28 and 1.34), indicating gradual desaturation and a more homogeneous pore network.

The difference in the shape of the curves between mature and young residual soils is associated with the degree of weathering and pedogenetic processes, as mature soils develop more complex structures due to prolonged exposure to weathering agents, which leads to bimodal characteristics (Gomes et al., 2023; Qian et al., 2022). On the other hand, young soils tend to retain characteristics of the parent rock, resulting in a less aggregated structure and typically unimodal behavior (Gomes et al., 2023).

The behavior of SWRCs in tropical soils deserves attention due to their unconventional shape. Hodnett &

Tomasella (2002) emphasized that the shape of the retention curve is mainly controlled by soil structure. In this regard, Delcourt et al. (2022) showed that the progressive advancement of weathering in tropical soils directly affects clay mineralogy, resulting in a higher fine fraction and a consequent increase in the second air-entry value of SWRC.

3.2 SWRC estimated by MIP

The SWRCs estimated by MIP (Figure 4) are consistent with the previous discussion, as they presented two air-entry values for GJM and SVM, typical of soils with dual structure (Gens et al., 1995; Khalili & Valliappan, 1996; Koliji et al., 2006), and gradual continuous desaturation for GJY and SVY, which have a single structure (Zhuang et al., 2024). Table 3 shows the van Genuchten adjustment parameters (dual-VG and VG) for MIP method, separated into mature and young residual soils, respectively.

The curve estimated by MIP showed a higher volumetric water content at saturation for all soils. For instance, according to Table 2 and Table 3, θ_s increased from 46.9% to 48.6% in GJM, from 49.2% to 65.7% in SVM, and from 47.5% to 71.8% in GJY, while SVY showed the largest discrepancy, rising from 38.0% to 63.6%. Regarding desaturation, all soils experienced water loss at lower suction values in the macropore region. For the micropores, this loss occurred at higher suctions in the mature residual soils.

However, a more pronounced difference in the shape of the curve was observed in the intermediate portion, between 10 and 10,000 kPa, similar to the results obtained by Motta et al. (2025). Delcourt et al. (2022) also observed this effect when comparing SWRCs from conventional tests and those derived from MIP, particularly in the meso- and macropore range, reporting that mercury intrusion pressure can affect the structure of residual soils. Additionally, Motta (2016) states that the mercury intrusion technique considers a non-polar fluid, which excludes adsorption phenomena, and that only interconnected pores in the soil are reached by this method, influencing the resulting total porosity.

According to Mendes & Marinho (2020), this discrepancy may be attributed to three main factors: the sample preparation process for MIP, the assumption of 100% saturation in porosimetry, and drying of the samples for MIP, which may cause variations in the specimen volume.

3.3 SWRC estimated by pedotransfer functions

M The model obtained using PTF-SV (Figure 4 and Table 3) showed variable performance, strongly dependent on soil structure. For the young unimodal soils (GJY and SVY), the prediction tended to overestimate the water retention capacity, as evidenced by the lower value of the parameter α compared to the experimental fit, since this parameter is inversely proportional to the air-entry pressure. This indicates

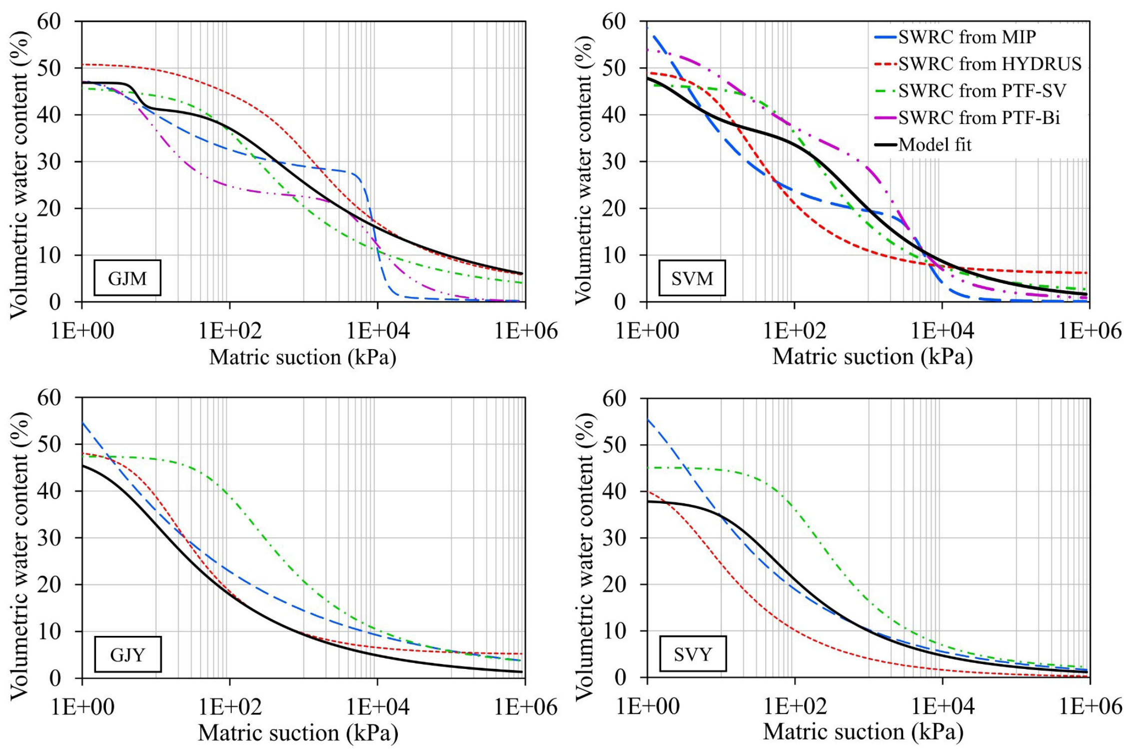

Figure 4. Water retention curves measured, fitted (Model Fit), and estimated by MIP, PTF-SV, PTF-Bi and HYDRUS for the studied soils (GJM, SVM, GJY, and SVY).

Table 3. van Genuchten model fitting parameters obtained from MIP, PTF-SV, PTF-Bi and HYDRUS data.

Soils	θ_s (%)	θ_r (%)	w_1	α_1	n_1	α_2	n_2
				MIP			
GJM	48.61	0.00	0.461	3.40E-01	1.36	1.14E-04	6.10
SVM	65.73	0.00	0.737	7.51E-01	1.47	1.97E-04	3.31
GJY	71.83	0.00	-	3.33E+00	1.20	-	-
SVY	63.60	0.00	-	9.33E-01	1.27	-	-
				PTF-SV			
GJM	55.49	0	0.303	1.36E+05	1.07	1.19E-02	1.35
SVM	49.99	0	0.161	4.96E+04	1.05	1.14E-02	1.46
GJY	47.41	2.14	-	1.15E-02	1.36	-	-
SVY	45.12	1.53	-	1.08E-02	1.45	-	-
				PTF-Bi			
GJM	47.45	0	0.525	1.54E-01	1.88	1.60E-04	1.98
SVM	54.48	0	0.551	1.64E-01	1.30	5.03E-04	2.16
				HYDRUS			
GJM	50.86	2.23	0.605	1.59E-03	1.42	5.54E-02	1.20
SVM	49.33	6.04	0.996	8.46E-02	1.49	1.22E-01	1.44
GJY	48.63	5.06	-	1.14E-01	1.48	-	-
SVY	42.50	0.01	-	3.58E-01	1.40	-	-

that the model predicts desaturation at higher suctions than those observed experimentally.

On the other hand, when applied to mature bimodal soils (GJM and SVM), the model failed to identify the macropore domain, responsible for the initial desaturation at low suction values, resulting in unrealistic α_1 values. This failure means that the PTF-SV treated the structure of these soils as unimodal, being unable to recognize the first desaturation step, which is characteristic of bimodality. Nevertheless, the model was able to closely approximate the SWRC behavior in the second desaturation phase (α_2 and n_2), demonstrating that the prediction can, to some extent, capture the micropore behavior.

Singh & Verdi (2024) emphasize that generalizing a model is a challenge under varying soil conditions, as is the case for tropical residual soils. Furthermore, the PTF-SV was developed based on international soils and Turkish data, without considering the structural peculiarities typically found in mature residual soils.

In this sense, the PTF-Bi model, developed specifically to represent bimodal soils based on Brazilian datasets, was able to capture the two distinct air-entry points for GJM and SVM. For both soils, the prediction of the initial air-entry value was efficient; however, it is worth highlighting the very close α_1 value of the GJM soil (1.54E^{-01}) to that of its Model Fit (1.81E^{-01}). In contrast, the model showed poorer performance in representing the micropore behavior when compared to PTF-SV, with an overestimation of the water retention capacity of these pores, as evidenced by the SWRC shifted to higher suctions in the second desaturation stage.

The efficiency of the approach based on tropical regions lies in its consideration of particle aggregation. According to the authors, fine particles present in weathered regions group together to form aggregates, resulting in larger pores between these aggregates (macropores), in addition to the micropores already present in the medium, leading to two or three distinct desaturation stages. This bimodal behavior is unlikely to be reproduced by models that do not account for it. To incorporate this effect, PTF-Bi considers two distinct states of particle-size distribution: disaggregated (with defloculant) and aggregated (without deflocculant). Based on these two behaviors, the neural network captures the nature of aggregation, reflecting bimodality more accurately in the curves, as it accounts for the degree of weathering in these soils (Pereira et al., 2024; Alves et al., 2025; Camapum de Carvalho & Gitirana Junior, 2021).

3.4 SWRC estimated by inverse modeling

Figure 4 summarizes the comparative curves between inverse modeling with HYDRUS-1D and the Model Fit (from laboratory measurements) for the different profiles. Table 3 presents the van Genuchten parameters obtained from HYDRUS-1D for each soil.

For the GJM soil, discrepancies were observed up to suctions of 10,000 kPa, after which high convergence occurred. In this high suction range, no laboratory measurements reached these values; therefore, the Model Fit is estimated without reference, increasing its uncertainty.

The GJY soil showed better convergence within the range of 100 to 5,000 kPa. However, outside this range, whether at lower or higher suctions, there was a consistent upward shift of about 5% in water content, indicating that HYDRUS tends to overestimate water content at more extreme suctions.

For the SVM soil, similar to GJY, HYDRUS-1D diverged from the Model Fit at low suctions (<10 kPa) and high suctions (>10,000 kPa), also overestimating water content. In intermediate suctions, the model underestimated water content, with differences exceeding 10%. At the end of the curve, in the high suction range, the behavior was similar to GJM.

The SVY soil exhibited similar behavior to the other soils. It initially overestimated water content, but this effect was almost negligible; from 2 kPa onward, HYDRUS-1D underestimated water content compared to Model Fit, showing intermediate behavior similar to SVM.

In summary, for some soils such as GJM, the HYDRUS estimated curves were more similar to the laboratory results, although inaccuracies were observed in all low-suction ranges (<10 kPa). This can be explained by Zhuang et al. (2024), who reported that the model performs better in soils with low macroporosity, where pore connectivity has less influence on water retention. Suction ranges from 1 to 10 kPa are predominantly influenced by macropores.

Additionally, the discrepancies observed between experimental data and the HYDRUS-1D estimates at low suctions can be partially attributed to hysteresis effects. The in situ data used for inverse modeling reflect both wetting and drying cycles, resulting in a retention curve that represents an intermediate hydraulic condition. In contrast, laboratory methods applied in this study characterize only the drying path. According to Kool & Parker (1987), drying paths generally exhibit higher water retention at a given suction compared to wetting paths due to air entrapment, pore connectivity, and differences in pore-scale drainage and filling mechanisms. Hysteresis was not explicitly incorporated in the inverse modeling, a limitation also acknowledged in similar HYDRUS-based studies (Singh & Verdi, 2024).

3.5 Model performance assessment

Statistically, Table 4 indicates that PTF-SV achieved the best performance for the mature residual soils (GJM and SVM), presenting low RMSE (0.032 and 0.031 $cm^3\ cm^{-3}$) and MAE values (0.027 and 0.024 $cm^3\ cm^{-3}$), high correlation coefficients (R = 0.99), and minimal bias (MBE = −0.021 for GJM and 0.004 for SVM). However, despite its strong statistical agreement, the model was not able to represent the dual structural behavior of these soils.

In contrast, PTF-Bi, although developed using Brazilian bimodal soils, showed higher RMSE values (0.065 for GJM and 0.055 for SVM), being the worst-performing model for GJM. This suggests that its training dataset may not fully represent the structural variability of these soils, limiting its generalization capacity.

Inverse modeling with HYDRUS showed promising results, being the second-best performing model. Despite higher errors (RMSE = 0.050 and 0.061), high correlation coefficients (R = 0.99 and 0.95) confirm its ability to capture retention dynamics, although it does not explicitly represent bimodal behavior. MBE values indicate overestimation for GJM (0.039) and underestimation for SVM (-0.019).

Similarly, MIP presented discrepancies. Despite a high correlation (R = 0.96), it yielded notable errors (RMSE = 0.058 and 0.075). The negative MBE for GJM (-0.024) suggests underestimation of water content across much of the suction range.

Overall, the models showed comparable predictive capacity, with high correlations (0.95-0.99). While effective in capturing moisture trends, significant methodological deviations remain.

Table 4. Accuracy of models for estimating the volumetric water content in mature residual soils.

Soils		MIP	PTF-SV	PTF-Bi	HYDRUS
GJM	RMSE	0.058	0.032	0.065	0.05
	MAE	0.047	0.027	0.051	0.041
	MBE	-0.024	-0.021	-0.05	0.039
	R	0.96	0.99	0.97	0.99
SVM	RMSE	0.075	0.031	0.055	0.061
	MAE	0.06	0.024	0.047	0.045
	MBE	-0.002	0.004	0.037	-0.019
	R	0.96	0.99	0.99	0.95
GJY	RMSE	0.076	0.107	-	0.029
	MAE	0.06	0.083	-	0.024
	MBE	-0.06	-0.083	-	0.023
	R	0.99	0.92	-	1
SVY	RMSE	0.095	0.076	-	0.064
	MAE	0.053	0.061	-	0.05
	MBE	0.044	0.061	-	-0.045
	R	0.95	0.97	-	0.96

The results for the young soils (Table 4) revealed a clear inversion in methodological performance, with HYDRUS providing the most accurate estimates. For GJY, it achieved an excellent fit (RMSE = 0.029, R = 1.00), and for SVY it also outperformed the other methods (RMSE = 0.064). This confirms the effectiveness of inverse modeling in representing in situ hydraulic behavior in structurally simpler soils. Bias analysis indicated slight overestimation for GJY (MBE = 0.023) and underestimation for SVY (MBE = −0.045).

MIP showed intermediate and inconsistent performance, being the second-best method for GJY but with strong underestimation (MBE = −0.060), and the least accurate for SVY (RMSE = 0.095; MBE = 0.044). This variability suggests that pore size distribution derived from mercury intrusion does not always directly correspond to water retention behavior. PTF-SV, previously effective for bimodal soils, showed the poorest performance for unimodal soils, particularly GJY (RMSE = 0.107; MBE = −0.083).

A regional pattern was also observed: Guarujá soils tended toward systematic underestimation, possibly reflecting pore features not well captured by the models, whereas São Vicente soils exhibited more controlled and variable bias, consistent with a more uniform pore structure.

4. Conclusions

This study addressed the estimation of the soil water retention curve in young and mature residual soils from the Baixada Santista region using different methods previously reported in the literature. The results demonstrated that no single method consistently outperforms the others across all soil types, as model performance strongly depends on soil structure and calibration data quality.

Although several methods showed strong statistical agreement with laboratory data, this agreement did not necessarily correspond to physically consistent parameterization. In several cases, fitted van Genuchten parameters were different among methods, leading to distinct interpretations of air-entry values and pore-domain contributions. This indicates that accurate curve fitting does not guarantee a realistic representation of the underlying pore structure and hydraulic processes.

Therefore, the selection of an estimation method must consider not only statistical indicators but also the physical consistency of the fitted parameters. The findings highlight the need for the development of tailored methods for Brazilian residual soils, especially those with more complex structures.

Acknowledgements

This research was funded by FAPESP, grant numbers 2023/04461-4, 2023/13865-1, 2023/13949-0 and by Finep, Invitation Letter MCTI/FINEP/FNDCT 01/2016, contractual instrument code No. 0.1.16.0068.00.

Declaration of interest

The authors have no conflicts of interest to declare. All co-authors have observed and affirmed the contents of the paper and there is no financial interest to report.

Authors' contributions

João Vitor Almeida Leite: Conceptualization, Data curation, Visualization, Writing – original draft. Vinícius Samahá Salles: Conceptualization, Data curation, Visualization, Writing – original draft. Mariana Ferreira Benessiuti Motta: Conceptualization, Data curation, Methodology, Supervision, Funding acquisition, Project administration, Validation, Writing – original draft. Marcio Roberto Magalhães de Andrade: Conceptualization, Formal Analysis, Funding acquisition, Project administration, Validation, Writing – review & editing. Daniel Metodiev: Validation, Writing – review & editing.

Data availability

The datasets generated analyzed in the course of the current study are available from the corresponding author upon request.

Declaration of use of generative artificial intelligence

This work was prepared with the assistance of generative artificial intelligence (GenAI) ChatGPT by OpenAI to improve language and readability in the writing process. The entire process of using this tool was supervised, reviewed and when necessary edited by the authors. The authors assume full responsibility for the content of the publication that involved the aid of GenAI.

List of symbols

dual-VG	dual-porosity van Genuchten model
e	void ratio / mean of the estimated volumetric water content values
h	matric potential
m	parameter that defines the curve shape / mean of the measured volumetric water content values
m_1, m_2	parameters that define the shape of the bimodal curve
n	porosity / parameter that defines the curve shape/ intruded porosity / number of observations
n_0	total soil porosity
n_1, n_2	parameters that define the shape of the bimodal curve
p	pressure value
u_s	suction for water
w	water content

w_1, w_2 weighting factors associated with macropore and micropore domains
w_L liquidity limit
w_P plasticity limit
w_r hygroscopic water content
w_s water content corresponding to the total saturation of the soil sample
CEMADEN National Center for Monitoring and Early Warning of Natural Disasters
D pore diameter
D* pore diameter (for mercury)
DCPs Data Collection Platforms
G relative density of grains
GJM Guarujá – Mature residual soil
GJM Guarujá – Mature residual soil
GJY Guarujá – Young residual soil
Ks saturated hydraulic conductivity
MAE Mean Absolute Error
MBE Mean Bias Error
MIP Mercury Intrusion Porosimetry
ML silt with low plasticity
NM not measured
NP non-plastic
PCNN-PTF Pseudo-Continuous Neural Network Pedotransfer Function
PTF-Bi Pedotransfer Function (Pereira et al., 2024)
PTF-SV Pedotransfer Function (Singh & Verdi, 2024)
PTFs Pedotransfer Functions
ReLU Rectified Linear Unit
RMSE Root Mean Square Error
S saturation degree
Se effective water saturation
SM silty sand
S_r degree of saturation
Sr_{nw} non-wetting fluid saturation
SV São Vicente
SVM São Vicente – Mature residual soil
SVY São Vicente – Young residual soil
SWRC Soil Water Retention Curve
T_{nw} surface tension (for mercury)
T_w surface tension
USCS Unified Soil Classification System
VG van Genuchten
V_{inj} volume of mercury injected per unit mass
VWC Volumetric Water Content
α parameter that defines the curve shape
α_1, α_2 parameters that define the shape of the bimodal curve
γ_d dry unit weight
θ volumetric water content
θ_e estimated volumetric water content
θ_m measured volumetric water content
θ_{nw} contact angle (for mercury)
θ_r residual water content
θ_s saturated water content
θ_w contact angle
ρ apparent specific mass
ρ_d apparent dry specific mass
ρ_s specific particle mass
φ mean grain/pore diameter

References

ABNT NBR 6459. (2016a). *Soil—Determination of the liquid limit*. ABNT—Associação Brasileira de Normas Técnicas, Rio de Janeiro (in Portuguese).

ABNT NBR 7180. (2016b). *Soil—Determination of the plastic limit*. ABNT—Associação Brasileira de Normas Técnicas, Rio de Janeiro (in Portuguese).

ABNT NBR 6502. (2022). *Soils and Rocks—Terminology*. ABNT—Associação Brasileira de Normas Técnicas, Rio de Janeiro (in Portuguese).

ABNT NBR 7181. (2025a). *Soil—Granulometric analysis*. ABNT—Associação Brasileira de Normas Técnicas, Rio de Janeiro (in Portuguese).

ABNT NBR 17212. (2025b). *Soils—Determination of the specific mass of solids in the fraction passing through a 2,0 mm aperture sieve*. ABNT—Associação Brasileira de Normas Técnicas, Rio de Janeiro (in Portuguese).

Albuquerque, E.A.C., Borges, L.P.F., Cavalcante, A.L.B., & Machado, S.L. (2022). Prediction of soil water retention curve based on physical characterization parameters using machine learning. *Soil and Rocks*, 45(3), 1-12. https://doi.org/10.28927/SR.2022.000222.

Alves, R.D., Gitirana Junior, G.F.N., & Vanapalli, S.K. (2025). Modeling the bimodal SWCC of highly weathered tropical soils using grain-size information. *Engineering Geology*, 351, 108031. https://doi.org/10.1016/j.enggeo.2025.108031.

ASTM ASTM D5298-16. (2016). *Standard Test Method for Measurement of Soil Potential (Suction) Using Filter Paper*. ASTM International, West Conshohocken, PA.

Aung, K.K., Rahardjo, H., Leong, E.C., & Toll, D.G. (2001). Relationship between porosimetry measurement and soil-water characteristic curve for an unsaturated residual soil. *Geotechnical and Geological Engineering*, 19(3-4), 401-416. https://doi.org/10.1023/A:1013125600962.

Bittelli, M., & Flury, M. (2009). Errors in water retention curves determined with pressure plates. *Soil Science Society of America Journal*, 73(4), 1453-1460. https://doi.org/10.2136/sssaj2008.0082.

Camapum de Carvalho, J., & Gitirana Junior, G.F.N. (2021). Unsaturated soils in the context of tropical soils. *Soil and Rocks*, 44(3), e2021068121. https://doi.org/10.28927/SR.2021.068121.

Delcourt, R.T., de Campos, T.M.P., & Antunes, F.S. (2022). Interrelationship among weathering degree, pore distribution and water retention in an unsaturated gneissic residual soil. *Engineering Geology*, 299, 106570. https://doi.org/10.1016/j.enggeo.2022.106570.

Durner, W. (1994). Hydraulic conductivity estimation for soils with heterogeneous pore structure. *Water Resources Research*, 30(1), 211-223. https://doi.org/10.1029/93WR02676.

Filipović, V., Weninger, T., Filipović, L., Schwen, A., Bristow, K.L., Zechmeister-Boltenstern, S., & Leitner, S. (2018). Inverse estimation of soil hydraulic properties and water repellency following artificially induced drought stress. *Journal of Hydrology and Hydromechanics*, 66(2), 170-180. https://doi.org/10.2478/johh-2018-0002.

Fredlund, D.G., & Xing, A. (1994). Equations for the soil-water characteristic curve. *Canadian Geotechnical Journal*, 31(4), 521-532. https://doi.org/10.1139/t94-061.

Gens, A., Alonso, E.E., Suriol, J., & Lloret, A. (September, 1995). Effect of structure on the volumetric behavior of a compacted soil. In *Proceedings of the 1st International Conference on Unsaturated Soils* (Vol. 1, pp. 83-88). Paris, France.

Gomes, F.S., Motta, M.F.B., Bernardes, G.P., & Soares, P.V. (2023). Influence of coconut fiber on the microstructural, mechanical and hydraulic behaviour of unsaturated compacted soil. *Soil and Rocks*, 46(2), e2023013322. https://doi.org/10.28927/SR.2023.013322.

Haghverdi, A., Oztürk, H.S., & Durner, W. (2018). Measurement and estimation of the soil water retention curve using the evaporation method and the pseudo continuous pedotransfer function. *Journal of Hydrology (Amsterdam)*, 563, 251-259. https://doi.org/10.1016/j.jhydrol.2018.06.007.

Hodnett, M.G., & Tomasella, J. (2002). Marked differences between van Genuchten soil water-retention parameters for temperate and tropical soils: a new water-retention pedotransfer function developed for tropical soils. *Geoderma*, 108(3-4), 155-180. https://doi.org/10.1016/S0016-7061(02)00105-2.

Ket, P., Oeurng, C., & Degré, A. (2018). Estimating soil water retention curve by inverse modelling from combination of in situ dynamic soil water content and soil potential data. *Soil Systems*, 2(4), 55. https://doi.org/10.3390/soilsystems2040055.

Khalili, N., & Valliappan, S. (1996). Unified theory of flow and deformation in double porous media. *European Journal of Mechanics. A, Solids*, 15(2), 321-336.

Koliji, A., Laloui, L., Cusinier, O., & Vulliet, L. (2006). Suction induced effects on the fabric of a structured soil. *Transport in Porous Media*, 64(2), 261-284. https://doi.org/10.1007/s11242-005-3656-3.

Kool, J.B., & Parker, J.C. (1987). Development and evaluation of closed-form expressions for hysteretic soil hydraulic properties. *Water Resources Research*, 23(1), 105-114. https://doi.org/10.1029/WR023i001p00105.

Le Bourgeois, O., Bouvier, C., Brunet, P., & Ayral, P.-A. (2016). Inverse modeling of soil water content to estimate the hydraulic properties of a shallow soil and the associated weathered bedrock. *Journal of Hydrology*, 541(Pt A), 116-126. https://doi.org/10.1016/j.jhydrol.2016.01.067.

Maček, M., Smolar, J., & Petkovšek, A. (September, 2013). Extension of measurement range of dewpoint potentiometer and evaporation method. In *Proceedings of the 18th International Conference on Soil Mechanics and Geotechnical Engineering* (pp. 1137-1142). Paris, France. French Society for Soil Mechanics and Geotechnical Engineering (CFMS).

Mendes, R.M.M., & Marinho, F.A.M. (2020). Soil Water Retention Curves for Residual Soils Using Traditional Methods and MIP. *Geotechnical and Geological Engineering*, 38(5), 5167-5177. https://doi.org/10.1007/s10706-020-01354-x.

METER Group. (2025a). *Operation Manual HYPROP*. METER Group. Retrieved in October 22, 2025, from http://library.metergroup.com/Manuals/UMS/Hyprop_Manual.pdf

METER Group. (2025b).*WP4C Dew Point Potentio Meter Operator's Manual*. METER Group. Retrieved in October 22, 2025, from http://library.metergroup.com/Manuals/20588_WP4C_Manual_Web.pdf

Motta, M.F.B. (2016). *Caracterização Físico-Hídrico-Estrutural e Efeito do Aumento da Pressão do Ar na Resistência de Solos Tropicais Não Saturados* [Ph.D. thesis]. Pontifical Catholic University of Rio de Janeiro (in Portuguese).

Motta, M.F.B., de Campos, T.M.P., da Fonseca, A.J.P.V., & Bernardes, G.P. (2025). On effects of a sudden increase of atmospheric pressure on unsaturated tropical soils. *Canadian Geotechnical Journal*, 62(1), 1-16. https://doi.org/10.1139/cgj-2024-0395.

Ottoni, M.V., Ottoni Filho, T.B., Schaap, M.G., Lopes-Assad, M.L.R.C., & Rotunno Filho, O.C. (2018). Hydro physical database for Brazilian soils (HYBRAS) and pedotransfer functions for water retention. *Vadose Zone Journal*, 17(1), 170095. https://doi.org/10.2136/vzj2017.05.0095.

Pereira, S.A.S., Silva Junior, A.C., Mendes, T.A., Gitirana Junior, G.F.N., & Alves, R.D. (2024). Prediction of soil–water characteristic curves in bimodal tropical soils using artificial neural networks. *Geotechnical and Geological Engineering*, 42(4), 3043-3062. https://doi.org/10.1007/s10706-023-02716-x.

Prapaharan, S., Altschaeffl, A.G., & Dempsey, B.J. (1985). Moisture curve of compacted clay: mercury intrusion method. *Journal of Geotechnical Engineering*, 111(9), 1139-1143. https://doi.org/10.1061/(ASCE)0733-9410(1985)111:9(1139).

Priesack, E., & Durner, W. (2006). Closed-form expression for the multimodal unsaturated conductivity function. *Vadose Zone Journal*, 5(1), 121-124. https://doi.org/10.2136/vzj2005.0066.

Qian, J., Lin, Z., & Shi, Z. (2022). Experimental and modeling study of water-retention behavior of fine-grained soils with dual-porosity structures. *Acta Geotechnica*, 17(8), 3245-3258. https://doi.org/10.1007/s11440-022-01483-y.

Richards, L.A. (1931). Capillary conduction of liquids through porous mediums. *Physics*, 1(5), 318-333. https://doi.org/10.1063/1.1745010.

Romero, E., Gens, A., & Lloret, A. (1999). Water permeability, water retention and microstructure of unsaturated compacted Boom clay. *Engineering Geology*, 54(1-2), 117-127. https://doi.org/10.1016/S0013-7952(99)00067-8.

Satyanaga, A., Rahardjo, H., Zhai, Q., Moon, S.-W., & Kim, J. (2024). Modelling particle-size distribution and estimation of soil–water characteristic curve utilizing modified lognormal distribution function. *Geotechnical and Geological Engineering*, 42(3), 1639-1657. https://doi.org/10.1007/s10706-023-02638-8.

Schaap, M.G., Leij, F.J., & van Genuchten, M.T. (2001). Rosetta: a computer program for estimating soil hydraulic parameters with hierarchical pedotransfer functions. *Journal of Hydrology (Amsterdam)*, 251(3-4), 163-176. https://doi.org/10.1016/S0022-1694(01)00466-8.

Schindler, U., & Müller, L. (2017). Soil hydraulic functions of international soils measured with the Extended Evaporation Method (EEM) and the HYPROP device. *Open Data J. Agric. Res.*, 3(1), 10-16. https://doi.org/10.18174/odjar.v3i1.15763.

Seki, K., Toride, N., & van Genuchten, M.Th. (2023). Evaluation of a general model for multimodal unsaturated soil hydraulic properties. *Journal of Hydrology and Hydromechanics*, 71(1), 22-34. https://doi.org/10.2478/johh-2022-0039.

Serviço Geológico do Brasil - CPRM. (2006). *Geologia e recursos minerais do Estado de São Paulo*. São Paulo: CPRM – Serviço Geológico do Brasil.

Šimůnek, J., Wendroth, O., & van Genuchten, M.T. (1999). Estimating unsaturated soil hydraulic properties from laboratory tension disc infiltrometer experiments. *Water Resources Research*, 35(10), 2965-2979. https://doi.org/10.1029/1999WR900179.

Singh, A., & Verdi, A. (2024). Estimating the soil water retention curve by the HYPROP-WP4C system, HYPROP-based PCNN-PTF and inverse modeling using HYDRUS-1D. *Journal of Hydrology (Amsterdam)*, 639, 131657. https://doi.org/10.1016/j.jhydrol.2024.131657.

Singh, A., Haghverdi, A., Öztürk, H.S., & Durner, W. (2020). Developing pseudo-continuous pedotransfer functions for international soils measured with the evaporation method and the HYPROP system: I. The soil water retention curve. *Water (Basel)*, 12(12), 3425. https://doi.org/10.3390/w12123425.

Solone, R., Bittelli, M., Tomei, F., & Morari, F. (2012). Errors in water retention curves determined with pressure plates: effects on the soil water balance. *Journal of Hydrology (Amsterdam)*, 470-471, 65-74. https://doi.org/10.1016/j.jhydrol.2012.08.017.

Tomasella, J., Hodnett, M.G., & Rossato, L. (2000). Pedotransfer functions for the estimation of soil water retention in Brazilian soils. *Soil Science Society of America Journal*, 64(1), 327-338. https://doi.org/10.2136/sssaj2000.641327x.

van Genuchten, M.T. (1980). A closed-form equation for predicting the hydraulic conductivity of unsaturated soils. *Soil Science Society of America Journal*, 44(5), 892-898. https://doi.org/10.2136/sssaj1980.03615995004400050002x.

Zhuang, L., Bezerra Coelho, C.R., Hassanizadeh, S.M., & van Genuchten, M. (2017). Analysis of the hysteretic hydraulic properties of unsaturated soil. *Vadose Zone Journal*, 16(1), 1-9. https://doi.org/10.2136/vzj2016.11.0115.

Zhuang, L., Chen, H., Yan, P., Liang, X., Teixeira, W.G., van Genuchten, M.Th., & Lin, K. (2024). Unsaturated hydraulic property measurements of subtropical anthropogenic (purple) soils in China. *Vadose Zone Journal*, 23(4), e20367. https://doi.org/10.1002/vzj2.20334.